Süleyman Demirel Üniversitesi Fen Edebiyat Fakültesi Fen Dergisi
Süleyman Demirel University Faculty of Arts and Sciences Journal of Science
2021, 16(1): 200-215
DOI: 10.29233/sdufeffd.874611
Atıf için / For Citation: M. S. Çavuş, N. Şener, "Analysis of Relationship Between Some Disazo Dyes Derived from 2,4-Dihydroxyquinoline and Its Anticancer and DNA Binding Properties by Density Functional Theory", *Süleyman Demirel Üniversitesi Fen Edebiyat Fakültesi Fen Dergisi*, 16(1), 200-215, 2021.

2,4-Dihidroksikinolinden Türetilen Bazı Disazo Boyalar ile Antikanser ve DNA Bağlanma Özellikleri Arasındaki İlişkinin Yoğunluk Fonksiyonel Teorisi ile Analizi

M. Serdar ÇAVUŞ*[1], Nesrin ŞENER[2]

[1]*Department of Biomedical Engineering, Faculty of Engineering and Architecture, Kastamonu University, Kastamonu, Turkey*
[2]*Department of Chemistry, Science-Arts, Kastamonu University, Kastamonu, Turkey*

**yazışılan yazar e-posta: mserdarcavus@kastamonu.edu.tr*

(Alınış / Received: 04.02.2021, Kabul / Accepted: 05.05.2021, Yayımlanma / Published: 27.05.2021)

2,4-dihidroksi kinolin türevi diazo boyalarının bazı fiziksel ve kimyasal özellikleri teorik yöntemlerle incelenmiştir. Bileşiklerin solvatokromik davranışını ve absorpsiyonunu belirlemek için altı farklı çözücü kullanılmış ve deneysel veriler kuantum kimyasal hesaplamalardan elde edilen teorik verilerle karşılaştırılmıştır. Bileşiklerin geometrik, elektronik ve bazı kimyasal reaktivite parametrelerini elde etmek için DFT hesaplamaları yapılmıştır. Bileşiklerin elektronik özellikleri ile DNA bağlanma, HeLa ve PC3 kanser hücre hatlarına karşı sitotoksisite kapasitesi arasındaki ilişkiyi belirlemek için molekül içindeki atom, doğal bağ yörüngesi, durum yoğunluğu, kovalent olmayan etkileşim, Fukui fonksiyonu, elektron lokalizasyon fonksiyonu ve elektron delokalizasyon aralığı analizleri yapılmıştır. –Cl ve $–NO_2$ sübstitüentlerine sahip bileşiklerin daha yüksek DNA bağlanmasına ve daha yüksek antikanser etkisine sahip olduğu görülmüştür. Sübstitüentlerin pozisyonlarının yanı sıra bağlardaki elektron yoğunluğu, delokalizasyon indexi değerleri ve nükleofilik ve elektrofilik saldırı bölgelerinin dağılımının bileşiklerin raktivitelerini belirleyen önemli faktörler arasında olduğu görülmüştür. Ayrıca, daha iyi DNA bağlanma özelliği gösteren bileşiklerin HOMO enerjilerinin durum yoğunlukları diğer bileşiklere göre daha yüksek hesaplanmıştır.

Anahtar kelimeler: DNA bağlanma, Antikanser, DFT, NCI, ELF, AIM.

Analysis of Relationship Between Some Disazo Dyes Derived from 2,4-Dihydroxyquinoline and Its Anticancer and DNA Binding Properties by Density Functional Theory

Abstract: It was studied some physical and chemical properties of 2,4-dihydroxy quinoline derivative diazo dyes by theoretical methods. Six different solvents were used to determine the solvatochromic behavior and absorption of the compounds, and the experimental results were compared with the theoretical data obtained from quantum chemical calculations. DFT calculations were carried out to obtain the geometric, electronic and some chemical reactivity parameters of the compounds. The atom in molecule, natural bond orbital, density of state, non-covalent interaction, Fukui function, electron localization function, and electron delocalization range analyzes of the compounds were performed to determine the relationship between the electronic properties and the DNA binding capacity and the cytotoxicity against HeLa and PC3 cancer cell lines. It was observed that the compounds substituted with –Cl and $–NO_2$ had higher DNA binding and higher anticancer effect. Besides the positions of the substituents, the electron

M. Serdar ÇAVUŞ, mserdarcavus@kastamonu.edu.tr, ORCID: https://orcid.org/0000-0002-3721-0883
Nesrin ŞENER, nsener@kastamonu.edu.tr, ORCID: https://orcid.org/0000-0001-5370-6048

density in the bonds, the delocalization index values and the distribution of the nucleophilic and electrophilic attack sites are among the important factors determining the reactivity of the compounds. In addition, the HOMO energies of the compounds with better DNA binding properties were calculated higher than the other compounds.

Key words: DNA binding, Anticancer, DFT, NCI, ELF, AIM.

1. Introduction

Contrary to what is thought, synthetic dyes are known to be used in many fields such as textile [1], paper [2], cosmetics [3], food [4], plastic [5], and pharmaceutical [6-8]. Azo dyes constitute the largest and most diverse group in synthetic dyes class and have been the subject of many studies, especially in the fields of biology and pharmacology [9-12].

Azo dyes containing heterocyclic rings have been proven to have brighter and deeper hues compared to those containing benzene rings [13] and are still very important for applications such as polyester fibers, disperse dyes [14,15]. Heterocyclic azo compounds have recently found wide use in spectrophotometric analysis and are now considered one of the most important classes of chromogenic reagents [16]. In addition, dyes using 2-aminothiazole compounds having different substituents at the 4-position of analog derivatives as diazo components have been reported to show bathochromic shifts relative to similar dyes derived from benzenoid compounds [17-21]. Moreover, the presence of biological properties of the heterocyclic groups that bind to the dyes was also found to have an effect [22-24]. Biological effects of pyrazole [25], pyrimidine [26], thiadiazole [27], quinoline [28] derivatives have been studied by many researchers in the literature.

Among these heterocyclic groups, quinolines are quite remarkable [28,29], because they can chelate Fe(II) and Fe(III) and inhibit free radical production in the Fenton reaction and that quinolines can also intercalate DNA duplexes and react with free radicals to protect DNA from oxidative damage [30]. At the same time, the use of these compounds derivatives is quite common in anticancer activity assays in recent years [31-35]. Quinoline derivatives are also used in many areas other than biological applications as chemosensor [36-38], catalyzer [39], alkaloid [40].

As in the previous study, we synthesized 2,4-dihydroxy quinoline derivative disazo dyes and characterized by spectroscopic methods such as FT-IR and ^{1}H-NMR. Then UV-vis absorption properties of the compounds with various solvents, such as dimethyl sulfoxide (DMSO), dimethylformamide (DMF), Acetonitrile (ACN), CH_3OH (Methanol), CH_3COOH (Acetic acid), and $CHCl_3$ (chloroform) were also studied. The experimental data was supported by the quantum chemical calculations. Also, the data obtained from the experiments and calculations were analyzed, compared and interpreted.

Although there are studies in the literature using DFT on anticancer and DNA binding, the molecules have been theoretically examined in the studies, but no significant relationship has been established between the electronic and anticancer properties of the compounds [41-50]. In this study, a detailed *atom in molecule* (AIM), *natural bond orbital* (NBO), *density of state* (DOS), *non-covalent interaction* (NCI), *Fukui function*, *electron localization function* (ELF), and *electron delocalization range* (EDR) analysis of the compounds were done and the relationship between the electronic properties of these compounds and DNA binding capacity and the cytotoxicity against HeLa and PC3 cancer cell lines was investigated.

2. Material and Methods

In the previous work [29], the 2,4-dihydroxyquinoline derived disazo dyes, given in Scheme 1, were synthesized. Both spectral properties and DNA protection, antimicrobial, and anticancer activities of these compounds were investigated. It was

observed that **3h** and **3j** had high DNA binding capacity, and also showed cytotoxicity against HeLa and PC3 cancer cell lines.

The aim of this study is to reveal the relationship between the electronic properties and the DNA binding capacity and the cytotoxicity properties against HeLa and PC3 cancer cell lines of the compounds.

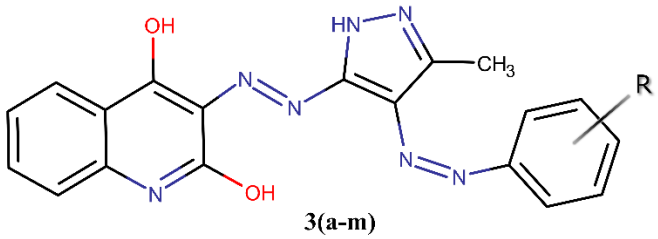

3(a-m)

R: **a.** -H **b.** *p*-NO_2 **c.** *p*-OCH_3 **d.** *p*-Cl **e.** *p*-CH_3 **f.** *m*-NO_2 **g.** *m*-OCH_3

h. *m*-Cl **i.** *m*-CH_3 **j.** *o*-NO_2 **k.** *o*-OCH_3 **l.** *o*-Cl **m.** *o*-CH_3

Figure 1. Synthesized quinoline derivative compounds.

2.1. Computational details

All calculations were performed by using the GAUSSIAN 09 [51] software package program. Kohn-Sham density functional theory (KS-DFT) [52,53] was used in the optimization process of the compounds without any geometric restriction. Molecular optimizations and spectral data calculations were performed by using Becke3-Lee-Yang-Parr hybrid exchange-correlation functional (B3LYP) [54,55] with cc-pvtz basis set. The Self-Consistent Reaction Area (SCRF) method and the Conductive Polarizable Sustainability Model (CPCM) were used under time-dependent density functional theory (TD-DFT) to calculate vertical excitation energies. The calculations were carried out in accordance with the experiment in dimethyl sulfoxide (DMSO), dimethylformamide (DMF), methanol, chloroform, acetic acid and acetonitrile phases.

Vibrational frequency calculations of the compounds were employed in the gas phase, and it was also determined that the compounds did not have imaginary frequencies, that is, the results correspond to the global minima on potential energy surfaces.

Proton nuclear magnetic resonance (^{1}H NMR) shifts of the compounds were computed by using the Gauge-Including Atomic Orbital (GIAO) method, in DMSO phase, using the conductor-like polarizable continuum model (CPCM).

FMO energy eigenvalues of the compounds were used to calculate electronic parameters such as energy gap (ΔE), chemical hardness (η) and electronegativity (χ).

Furthermore, Bader's theory of atoms in molecules (AIM) [56-58] analysis was carried out to determine the intramolecular interactions and electron charge distribution. The single point energy calculation of the compounds was performed at B3lyp/6-311++g(2d,2p) level, and used for DOS, NCI, Fukui function, ELF, and EDR analysis, in gaseous phase, at the same level of theory.

3. Results and Discussion

The relationship between the electronic properties of the compounds and DNA binding capacity and anticancer properties depends on the conformational structure of the compounds. The conformation of a compound directly affects the interaction of the

compound with the environment, because conformation determines many properties of the compound such as from the intramolecular interaction to the dipole moment, from the steric effect to the degree of freedom of the reactive regions. In the theoretical approaches, although intermolecular interactions can be partially performed in addition to single molecule calculations, the formations generated by molecule-environment interactions cannot be fully reflected in the results of the calculations. At this point, choosing the right conformer is of great importance. In the first step of the calculations, the compounds were sequentially scanned dihedrally and conformers with the lowest energy were obtained. Compounds were scanned using four dihedral rotors $D_{1\text{-}4}$, as given Figure 1, at b3lyp/3-21g levels of the theory.

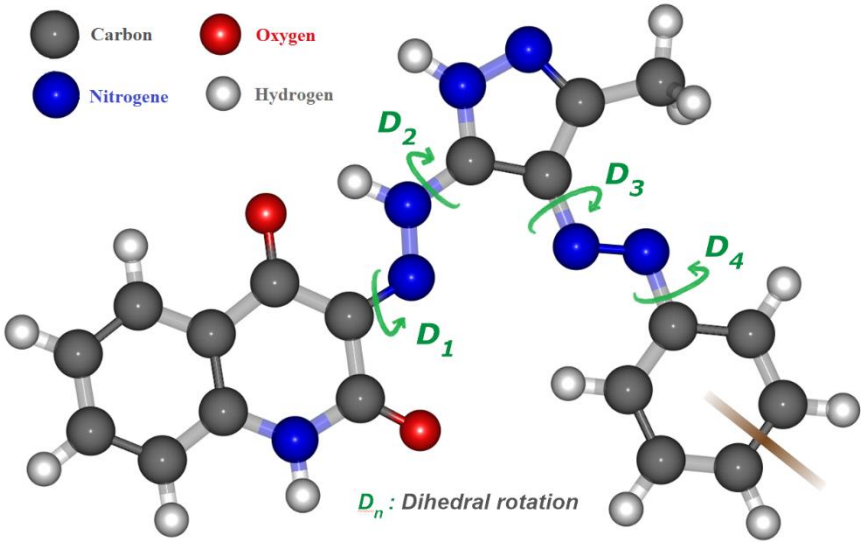

Figure 1. Dihedral scanning of the compounds.

Calculated electronic parameters of the compounds is given Table 1. The higher binding affinity of the –Cl and $–NO_2$ substituted compounds to the negatively charged DNA may be associated with their electronic properties. The molecular energies of the compounds at the *p*- position of their substituents were the lowest, while at the *o*-position they received the highest value. If the unsubstituted compound **3a** is taken as reference, it is seen that the effect of the substituted groups on the HOMO-LUMO energies of the compounds varies according to the structure of the substituent. It was observed that the –Cl and $–NO_2$ substituents decreased both HOMO and LUMO energies, while the $–CH_3$ and $–OCH_3$ substituents increased. Both the HOMO and LUMO energies of the –Cl and $–NO_2$ substituted compounds were calculated lower than the other compounds. The HOMO-LUMO energy gap ΔE was calculated as the largest for $–NO_2$ substituted compounds and the smallest for $–OCH_3$ substituted compounds. The inductive effects of $–NO_2$ and –Cl substituents are greater than that of other substituents.

Table 1. Electronic parameters of the compounds, calculated by 6-311++g(2d,2p) basis set.

Comp.	*Subs.*	*E* (kJ mol^{-1})	E_{HOMO} (eV)	E_{LUMO} (eV)	Δ*E*	*η* (eV)	*χ* (eV)	*μ (Debye)*	*α (a,u,)*
3a	–H	-3326755.98	-6.158	-3.339	2.819	1.409	4.748	4.685	362.909
3j	*o*-NO_2	-3863822.01	-6.417	-3.398	3.019	1.509	4.908	4.057	369.954
3f	*m*-NO_2	-3863851.42	-6.470	-3.533	2.937	1.469	5.001	0.767	377.519
3b	*p*-NO_2	-3863853.32	-6.587	-3.717	2.870	1.435	5.152	6.032	393.815
3l	*o*-Cl	-4533481.20	-6.233	-3.363	2.871	1.435	4.798	3.694	378.979
3h	*m*-Cl	-4533499.91	-6.296	-3.428	2.868	1.434	4.862	2.940	375.234
3d	*p*-Cl	-4533501.47	-6.217	-3.432	2.785	1.392	4.825	4.061	385.946

3m	*o*-CH_3	-3430005.79	-6.116	-3.357	2.759	1.379	4.737	4.865	381.672
3i	*m*-CH_3	-3430015.50	-6.116	-3.319	2.797	1.399	4.718	5.092	376.270
3e	*p*-CH_3	-3430016.55	-6.036	-3.289	2.748	1.374	4.662	5.122	383.548
3k	*o*-OCH_3	-3627517.87	-5.892	-3.245	2.647	1.323	4.569	6.062	387.449
3g	*m*-OCH_3	-3627535.14	-6.052	-3.376	2.675	1.338	4.714	5.086	381.890
3c	*p*-OCH_3	-3627539.32	-5.835	-3.240	2.595	1.297	4.538	6.415	396.116

E: Molecular energy, $\boldsymbol{E_{HOMO}}$: HOMO energy, $\boldsymbol{E_{LUMO}}$: LUMO energy, $\Delta\mathbf{E} = E_{LUMO} - E_{HOMO}$, $\boldsymbol{\eta}$: Chemical hardness, $\boldsymbol{\chi}$: Electronegativity, $\boldsymbol{\mu}$: Dipol moment, $\boldsymbol{\alpha}$: Polarizability.

Moreover, it can be said that the higher number of "lone pair electrons" of the $–NO_2$ and –Cl substituents contribute to their ability to react with the environment. Polarizability is affected from the intra- and intermolecular interactions, and plays an important role in determining the spectroscopic signatures of molecules. It was observed that the polarizability of the compounds varies with the positions of the substituents, and the polarizability of the *o*-NO_2 and *m*-Cl substituted compounds is calculated lower than the other positions of the substituents.

AIM, NBO, DOS, FUKUI, and EDR analysis of the compounds

Analysis of charge distributions based on the positions of the substituents can be a consistent approach to obtain meaningful data on both DNA binding and anticancer properties of compounds. The charge distribution on the substituted groups is highly influenced by intramolecular interactions, and so, it was seen that the distribution is strongly dependent on the position of substituents and electronegativity (the *o*-, *m*-, and *p*- positions).

AIM analysis revealed how the resonance or inductive effect of the substituents and the phenyl ring is affected by intramolecular interactions, but also gave significant results in determining the possible structure of the molecule-environment interaction. Intramolecular interactions have caused the charge distribution of the substituents to change, and consequently to the change of the molecular charge distribution. AIM analysis data are given in Table 2.

Table 2. AIM data, calculated by B3LYP/6-311++g(2d,2p) method.

Comp.	Substituent	$DI^{(i)}$	$Rho^{(j)}$	T_{Rho}
3a	–H	-	-	0.406828
3j	*o*-NO_2	0.86795267245	0.260459	0.286918
3f	*m*-NO_2	0.86970528221	0.256793	0.317209
3b	*p*-NO_2	0.87876508916	0.260028	0.338629
3l	*o*-Cl	1.13245241050	0.193333	0.352528
3h	*m*-Cl	1.11165700380	0.187616	0.375987
3d	*p*-Cl	1.11934730990	0.189062	0.396131
3m	*o*-CH_3	1.02209132280	0.251065	0.384635
3i	*m*-CH_3	1.01282540030	0.249120	0.412680
3e	*p*-CH_3	1.01583830520	0.250145	0.424421
3k	*o*-OCH_3	0.94666699963	0.300499	0.402349
3g	*m*-OCH_3	0.92956218914	0.290977	0.408268
3c	*p*-OCH_3	0.93574722994	0.293343	0.453534

i*:** For the covalent bound between substituted group and C atom on the benzene ring, ***j: For the bond between the substituent and the phenyl ring, $\mathbf{T_{Rho}}$: Total charge of phenyl ring-including substituent.

AIM analysis revealed that when compared to the phenyl ring of the non-substituted compound **3a**, the total charge of the –Cl and $–NO_2$ substituted phenyl rings decreased relatively, while that of the methyl and methoxy substituted compounds increased. $–NO_2$ substituent is more electronegative than –Cl, and besides, the resonance effect of $–NO_2$ on the phenyl ring was greater than the inductive effect of –Cl, causing $–NO_2$

substituted compounds to be more reactive than –Cl substituted compounds. DNA binding and consequently anticancer effect was observed on –Cl and –NO_2 substituted compounds having higher electron density on the active phenyl ring. Moreover, the relative positions of the –C1 and –NO_2 substituents directly affect the DNA binding of these compounds. The *o*-NO_2 substituent caused an electron density greater than that of the *m*- and *p*- positions on the phenyl ring with the contribution of intramolecular interactions (Figure 2). Furthermore, for –C1 substituted compounds **3l**, **3h**, and **3d**, the electronegative nucleus of the chlorine withdraws electrons from the compound and thus causes a dipole moment by strongly polarizing the bond. The mesomeric/inductive effect on the phenyl ring occurs due to the polarization of the aromatic σ-bond framework by the –Cl. The Cl-substituent causes the mesomeric effect by donating the electron to the π system covering the σ-frame of the phenyl ring. The polarity resulting from the decrease of delocalized electrons as a result of the increase of localized electron causes the delocalization index (DI) to be smaller.

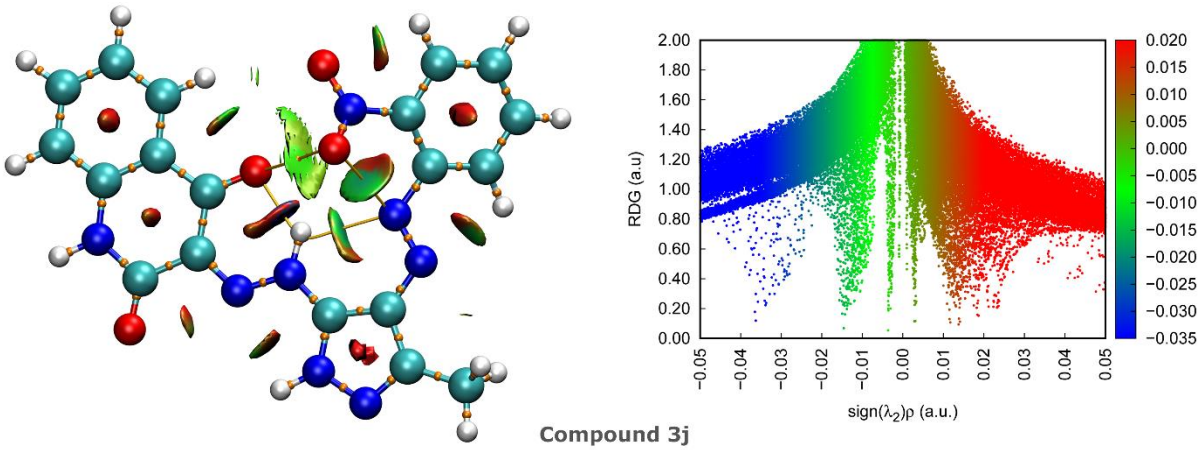

Figure 2. AIM and NCI maps of the compound **3j**.

The electron density (0.187616 au) and the delocalization index (1.1116570038) between the chlorine substituent and the phenyl ring were calculated lower in the *m*-position than *o*- and *p*- positions. However, in –NO_2 substituted compounds, the DI between the substituent and the phenyl ring was calculated as the lowest in the *o*-position, while the electron density was calculated as the highest. Also, the –NO_2 substituent caused strong intramolecular interaction at the *o*-position.

Furthermore, NBO analysis showed that the interaction of lone pair electrons with the phenyl ring resulted in increased electron density between the –NO_2 and the phenyl ring. Considering the donor-acceptor (bond-antibond) interactions of lone pair electrons on –Cl and –NO_2 substituted compounds, it was observed that the strongest stabilization between the lone pair NBOs of substituents and the related antibonds took place between adjacent atomic groups (Table 3). In addition, for the *o*-NO_2 substituted compound **3j** and the *m*-Cl substituted compound **3h**, the sum of the stabilization energies of both the 2-center antibond (BD*) and 1-center Rydberg (RY*) interactions of the lone pair NBOs was calculated as the lowest (54.78 kcal/mol for **3j**, 10.14 kcal/mol for **3h**). This indicates that *o*-NO_2 and *m*-Cl substituents in compounds **3j** and **3h** are more reactive than other substituents in their own group.

Table 3. Some NBO data of the NO_2 and Cl substituted compounds.

Comp.	Substutient	Donor NBO	Acceptor NBO	E(2) kcal/mol	E_s kcal/mol
3j	*o*-NO_2	LP O43	C32-N42	12.55	54.78
			N42-O44	9.00	
		LP O44	C32-N42	12.47	
			N42-O43	5.67	
3f	*m*-NO_2	LP O43	C34-N42	12.94	61.99
			N42-O44	6.20/6.83	
		LP O44	C34-N42	13.32	
				3.38	
3b	*p*-NO_2	LP O42	N41-O42	21.93	85.69
		LP O43	N41-O42	11.92	
3l	*o*-Cl	LP Cl42	C31-C32	14.2	30.1
3h	*m*-Cl	LP Cl43	C32-C34	4.23	10.14
3d	*p*-Cl	LP Cl41	C36-C38	8.71	23.25

E(2): stabilization energy, $\mathbf{E_s}$: Sum of stabilization energies (for LP to BD* and RY*), C(31-34): Carbon atoms where the substituents are attached to the phenyl ring, N(41,42)/O(42-44): Nitrogen and oxygen atoms of the substituents.

DOS analysis revealed that HOMO energies and state densities were particularly affected by the positions of the substituents (Figure 3). The state intensities of HOMO energy levels of the compounds showing better DNA binding property were higher compared to other compounds (Figure 3-b). In addition, low level HOMO energies (from HOMO-1 to HOMO-4) of $-NO_2$ and –Cl substituted compounds were also calculated lower than those of methyl and methoxy substituted compounds. In other words, the $-NO_2$ and –Cl substituted groups decrease the HOMO energies of the compound **3a** to which they are attached, while the methyl and methoxy substitute groups have increased the HOMO energies.

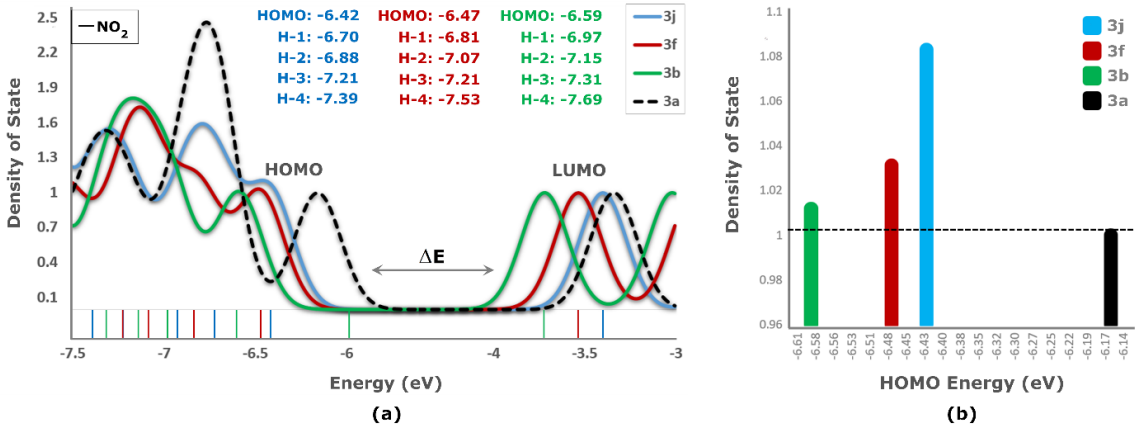

Figure 3. (a) DOS graph of compound **3j**. (b) HOMO energy versus DOS graph of compound **3j**.

The Fukui function is related to the change of electron density with respect to the number of electrons, and is also interpreted as a change in the chemical potential relative to the local external potential. The dual descriptor $\Delta f(r)$ is defined in terms of Fukui functions (f^- and f^+) and allows the nucleophilic and electrophilic attack sites to be examined at an ***r*** point in a molecular system. The electron delocalization range EDR(**r**,*d*) function determines the degree of delocalization of an electron at the ***r*** point in a calculated wave function along the distance *d*. Figure 4 shows how, for compound **3h**, the positions of the substituted groups affect electron delocalization and reactive sites for electrophilic and nucleophilic attack.

It was observed that the electron delocalization range of *m*-NO_2 and *p*-NO_2 substituted compounds was higher than that of compound **3j**. This situation caused intramolecular interactions in compounds **3f** and **3b** to be stronger than those of **3j** and made the interaction of the *o*-NO_2 compound with the environment easier. In addition, the electrophilic attack sites on the phenyl ring of compounds **3j** and **3b** (with *o*-NO_2 and *p*-NO_2) are wider than those of the *m*-NO_2 substituted compound **3f**, and these substituents are more favorable than the meta position for the nucleophilic attack. The *m*-Cl substituent also appears to strengthen the nucleophilic attack sites on the phenyl ring more than the *o*- and *p*- positions. In general, it can be said that compounds with larger nucleophilic attack sites show higher reactivity, and compounds whose EDRs contribute less to intramolecular interaction, or in other words, compounds with higher non-molecular EDRs (such as **3h** and **3d**) are also more reactive.

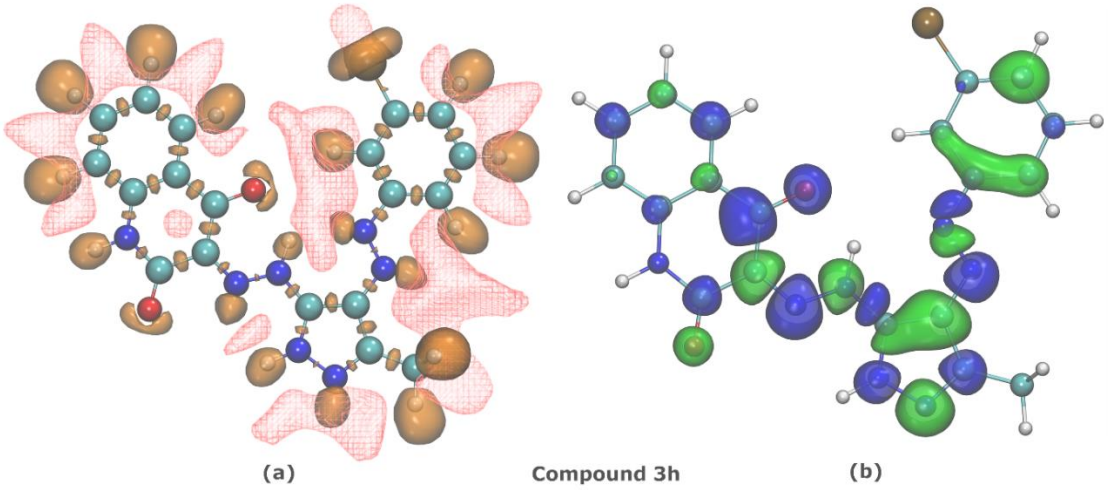

Figure 4. (a) ELF, and EDR maps of the compound **3h** (isovalue: 0.1 for EDR plotted by red grid, 1.68 for ELF colored by orange). (b) Green and blue surfaces correspond to electrophilic and nucleophilic behavior regions of $\Delta f(r)$, respectively (isovalue: 0.002 for dual descriptor).

UV-Vis absorption study of the compounds

In this study, we used six different solvents to determine the solvatochromic behavior of the dyes **3(a–m)** and the absorption spectrums of compounds were recorded between 10^{-8} and 10^{-6} M and over the range of λ between 300-700 nm. These solvents have different dielectric constants (ε) as follows: i.e. DMSO (ε: 46.45), DMF (ε: 36.71), ACN (ε: 35.94), CH_3OH (Methanol, ε: 32.66), CH_3COOH (Ascetic asit, ε: 6.17), and $CHCl_3$ (Chloroform, ε: 4.89) [59]. The effects of solvents on the UV absorption properties of the compounds were also analyzed by DFT calculations and the calculation results were compared with the experimental data. The experimental and theoretical absorption values of the compounds are summarized in Table 4.

Absorbance is a measure of the amount of light absorbed, and affected by the chemical composition, surrounding environment, solvent and temperature, concentration, and so on. However, it was observed that compounds with lower absorbance values were more active in DNA binding (see Figure 5).

Table 4. Influence of solvent on λ_{max} (nm) of dyes 3(a-m).

	Dyes	DMSO	DMF	Acetonitrile	Methanol	Acetic acid	Chloroform
Experimental	3a	322, 334, 450	321, 334, 429	320, 333, 424	313, 432	311, 322, 426	328, 496
	3b	232, 336, 363, 459	323, 336, 357, 455	352, 436s	314, 326, 364	312.5, 324, 360	316, 356
	3c	321, 335, 457	322, 334, 450	321, 335, 352s, 426	314, 325, 353s, 452	311, 322, 346, 437	352
	3d	322, 335, 453	322, 334, 450	322, 333.5, 420	314, 437	312, 322.5, 342s, 436	332, 344, 460
	3e	321, 334, 387, 457	322, 335, 450	320, 333.5, 420	314, 325, 349s, 443	311, 322.5, 345s, 432	333, 356s, 433
	3f	322, 335, 439	321, 334, 457	322, 332.5, 412s	313, 414, 480s	311, 322, 406	334, 426s
	3g	322, 335, 452	322, 335, 450	321, 333.5, 411.5	314, 326, 448	311.5, 322.5, 429	333, 352s, 436.5
	3h	322, 335, 452	323, 335, 452	322.5, 333.5, 421	314, 325, 346s, 438	311.5, 323, 345s, 425.5	333, 416
	3i	322, 335, 425	321, 335, 387, 421	321.5, 333.5, 411.5	314, 414	311.5, 322.5, 419.5	338, 436s
	3j	321, 335, 452	321, 334, 453	320, 333, 438	313, 325, 450	311, 322.5, 443	332, 485
	3k	321, 334, 429	321, 335, 429	318, 334s, 424	313, 425	310, 321s, 424	314, 333s, 426
	3l	321, 334, 446	321, 334, 446	322, 333, 404	314, 448	311.5, 322, 435	335, 478
	3m	334, 442	335, 446	329, 435	329, 453	326, 441	332, 478
Calculated	3a	336, 523	332, 515	331, 512	330, 512	332, 515	332, 518
	3b	312, 385, 527	307, 374, 518	373, 516	372, 516	373, 520	369, 515
	3c	348, 433, 571	343, 429, 561	341, 427, 558	341, 427, 557	342, 428, 559	342, 429, 561
	3d	341, 530	340, 522	336, 519	335, 519	337, 523	337, 525
	3e	339, 427, 538	334, 528	333, 525	333, 525	334, 527	335, 530
	3f	321, 505	313, 500	312, 490	315, 498	313, 493	314, 492
	3g	343, 543	322, 535	340, 533	317, 532	341, 537	321, 539
	3h	338, 522	330, 515	334, 512	322, 512	335, 516	325, 518
	3i	336, 526	320, 505	330, 515	330, 514	331, 518	331, 520
	3j	324, 484	317, 480	321, 479	313, 478	323, 482	324, 484
	3k	340, 516	338, 517	337, 516	337, 516	338, 520	339, 523
	3l	322, 514	327, 507	335, 512	334, 511	335, 515	336, 518
	3m	329, 420, 524	334, 423, 519	333, 516	332, 421, 516	334, 519	334, 424, 522

s: shoulder

In the table, it is seen that the dyes give more than one maximum absorption point in different solvents. According to the table it was observed that λmax of dyes **3(a-m)** shifted hypsochromically in all solvents from DMSO to acetic acid. For example, for the dye **3a** maximum absorption points are 322, 334, 450 nm in DMSO, 311, 322, 426 nm in acetic acid, for the dye 3c maximum absorption points are 321, 335, 457 nm in DMSO, 311, 322, 346, 437 in acetic acid. However, it is observed that λ_{max} of dyes in chloroform solvent shifted batochromically than in the DMSO solvent. It is understood that this is due to the oxygen and nitrogen atoms that contain nonbonding electron pairs in the molecular structures [60]. The reason why the compounds give more than one absorption point in different solvents is because of π-π * and n-π * electronic transitions due to π bonds, nonbonding electron pairs and conjugation in the structures of compounds. The first of these two absorption bands results from π-π * electronic transitions and the second from n-π * electronic transitions. This is due to the reduced polarity of the solvents causing low band gap in the n-π * electronic transitions and to the shift to lower energy [61]. In addition, the presence of shoulders along with absorption points in some dyes suggests that the compounds are not in a single tautomeric form.

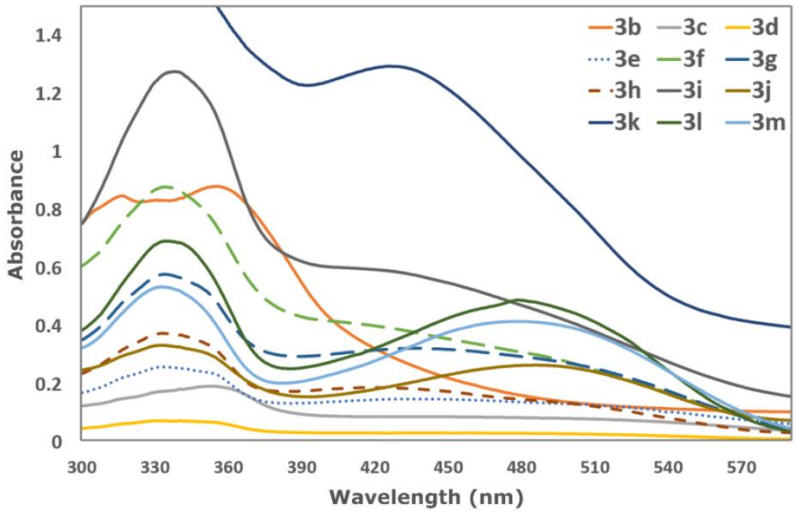

Figure 5. Experimental UV data of compounds.

FT-IR analysis of the compounds

IR calculations of the compounds were performed in the gaseous phase, and results is given in Table 5. Vibrational frequencies of N–H group were observed at 3650-3286 cm^{-1}, 3651-3303 cm^{-1}, 3652-3306 cm^{-1}, 3653-3305 cm^{-1} for $–NO_2$, –Cl, $–CH_3$, and $–OCH_3$ substituted groups, respectively. Stretching vibration of aromatic and aliphatic C–H were calculated for all compounds as 3233-3165 cm^{-1} and 3137-3033 cm^{-1}, respectively. Stretching vibration of C=O and N=N were obtained as 1746-1658 cm^{-1} and 1476-1446 cm^{-1}, respectively. Also, vibration of $C–OCH_3$ (compounds **3k**, **3g**, **3c**) was obtained as 1060-1053 cm^{-1}. Antisymmetric and symmetric stretching vibrations of the $–NO_2$ (compounds **3j**, **3f**, and **3b)** were calculated as 1569-1560 and 1373-1357 cm^{-1}, respectively. It was seen that the experimental data and the theoretical results were compatible.

Table 5. IR values of compounds, calculated by b3lyp/6-311++g(2d,2p) method.

	Comp.	$\nu_{NH\ (stretching)}$	$\nu_{Aromatic-H}$	$\nu_{Aliphatic-H}$	$\nu_{C=O}$	$\nu_{NH\ (bending)}$	$\nu_{N=N}$	ν_{NO2}	ν_{C-O}
	3a	3651 [a] 3605 [b] 3307 [c]	3214-3172	3133-3096	1744 [d] 1659 [e]	1532	1461	-	-
$–NO_2$	**3j**	3650 [a] 3605 [b] 3299 [c]	3223-3181	3135-3049	1746 [d] 1665 [e]	1534	1462	1568 1373	-
	3f	3650 [a] 3604 [b] 3286 [c]	3233-3173	3135-3049	1746 [d] 1659 [e]	1533	1446	1569 1369	-
	3b	3648 [a] 3604 [b] 3309 [c]	3211-3174	3136-3050	1748 [d] 1660 [e]	1533	1466	1560 1357	-
–Cl	**3l**	3645 [a] 3604 [b] 3353 [c]	3218-3171	3133-3048	1745 [d] 1665 [e]	1531	1454	-	-
	3h	3651 [a] 3605 [b] 3303 [c]	3221-3173	3134-3049	1745 [d] 1659 [e]	1532	1467	-	-
	3d	3651 [a] 3605 [b] 3307 [c]	3219-3173	3137-3049	1745 [d] 1659 [e]	1533	1469	-	-
$–CH_3$	**3m**	3648 [a] 3604 [b] 3350 [c]	3218-3165	3133-3049	1744 [d] 1660 [e]	1530	1454	-	-
	3i	3652 [a] 3605 [b] 3309 [c]	3217-3165	3133-3036	1744 [d] 1659 [e]	1532	1468	-	-
	3e	3652 [a] 3605 [b] 3306 [c]	3212-3166	3133-3033	1743 [d] 1659 [e]	1531	1470	-	-
$–OCH_3$	**3k**	3649 [a] 3605 [b] 3342 [c]	3217-3171	3132-3048	1743 [d] 1662 [e]	1531	1456	-	1053
	3g	3652 [a] 3605 [b] 3316 [c]	3223-3173	3133-3049	1744 [d] 1658 [e]	1532	1472	-	1060
	3c	3653 [a] 3606 [b] 3305 [c]	3217-3172	3132-3048	1742 [d] 1658 [e]	1531	1476	-	1054

a: pyrazole −NH, **b**: Quinoline −NH, **c**: Azo bridge −NH, **d**: Quinoline 2-substituted C=O, **e**: Quinoline 4-substituted C=O.

^{1}H NMR analysis of the compounds

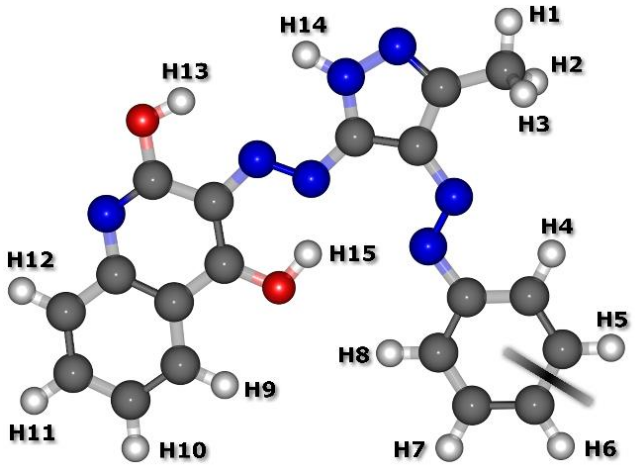

Figure 6. Numbering of the atoms on the compounds, for ^{1}H-NMR calculations.

Figure 6 is used to enumerate proton chemical shifts, and the calculated ^{1}H NMR data are given in Table 6. The ^{1}H NMR data reveal that the substituents influence the chemical shifts of the hydrogen atoms in the phenyl ring containing reactive substituents, ie the distribution of the charge on the reactive phenyl ring is more affected by the substituents than on the other parts of the compounds.

Table 6. ^{1}H NMR data of the compounds, calculated by b3lyp/cc-pvtz method.

Comp.	$\delta_{\text{Aliphatic-H}}$			$\delta_{\text{Aliphatic-H}}$ (*)			$\delta_{\text{Aromatic-H}}$									$\delta_{\text{X-H}}$		
	H1	**H2**	**H3**	**H1***	**H2***	**H3***	**H4**	**H5**	**H6**	**H7**	**H8**	**H9**	**H10**	**H11**	**H12**	**H13**	**H14**	**H15**
3a	2.7	3.0	3.0	-	-	-	8.5	8.0	8.1	8.2	9.0	8.9	8.0	8.3	8.1	8.8	10.7	15.8
3b	2.7	3.0	3.0	-	-	-	8.5	9.1	-	9.2	9.0	8.9	8.0	8.4	8.1	8.7	10.8	15.9
3c	2.6	2.9	2.9	4.5	4.1	4.1	8.5	7.5	-	7.6	8.8	8.9	8.0	8.3	8.1	8.7	10.6	15.7
3d	2.7	3.0	3.0	-	-	-	8.4	8.0	-	8.2	8.9	8.9	8.0	8.3	8.1	8.8	10.7	15.8
3e	2.7	3.0	3.0	2.9	2.9	2.4	8.4	7.8	-	8.0	8.9	8.9	8.0	8.3	8.1	8.8	10.7	15.7
3f	2.7	3.1	3.1	-	-	-	9.5	-	9.0	8.3	9.4	9.0	8.0	8.3	8.1	8.8	10.8	15.8
3g	2.7	3.0	3.0	4.3	4.0	4.0	7.9	-	7.6	8.0	8.5	8.9	8.0	8.3	8.1	8.8	10.7	15.7
3h	2.7	3.0	3.0	-	-	-	8.4	-	8.0	8.1	8.8	8.9	8.0	8.3	8.1	8.8	10.7	15.8
3i	2.7	3.0	3.0	2.8	2.8	2.4	8.3	-	7.9	80.	8.8	8.9	8.0	8.3	8.1	8.8	10.7	15.7
3j	2.6	2.7	2.8	-	-	-	-	8.2	8.0	8.3	8.5	8.8	7.9	8.3	8.1	8.8	10.8	15.4
3k	2.7	2.9	2.9	4.4	4.1	4.1	-	7.6	7.9	7.7	8.9	8.9	8.0	8.3	8.1	8.8	10.7	15.9
3l	2.7	3.1	2.9	-	-	-	-	8.0	7.8	8.0	8.2	8.7	7.9	8.3	8.1	8.8	10.8	15.3
3m	2.7	2.9	2.9	3.1	3.1	2.6	-	7.9	7.9	8.1	9.1	8.9	8.0	8.3	8.1	8.8	10.7	15.9

*: for substitute groups.

3. Conclusion and Comment

2,4-dihydroxy quinoline derivative diazo dyes were characterized by spectroscopic FT-IR and ^{1}H-NMR methods. In addition, the UV-vis absorption properties of the compounds in various solvents were also examined. Experimental spectroscopic data were supported by DFT calculations. In addition, electronic data obtained from AIM, NBO, DOS, NCI, Fukui, ELF and EDR calculations were analyzed and the results were used to predict the DNA binding capacity of the compounds and their cytotoxicity properties against HeLa and PC3 cancer cell lines.

It was observed that the –Cl and $–NO_2$ substituted compounds with higher electron density on the active phenyl ring have higher DNA binding and thus higher anticancer

effect. The relative positions of the –Cl and $–NO_2$ substituents determined the electron density on the phenyl ring and the degree of electron delocalization, thus directly affecting the DNA binding of the compounds. In addition to the substituent positions, electron density and DI values on the bonds are among the factors that determine the activities of the compounds. It has been found that the effectiveness of the nucleophilic and electrophilic attack sites of the compounds is affected by the position of the substituents, and the reactivity of the compounds changes accordingly. Moreover, the state densities of HOMO energies of compounds showing better DNA binding property were calculated higher than other compounds. It has also been observed that the low-level HOMO energies of the $–NO_2$ and –Cl substituted compounds are lower than the methyl and methoxy substituted compounds.

Considering all the data, it is concluded that the biological effects of the molecules depend on the electronic properties of the molecule in a multivariate, and that significant predictions can only be made regarding the reactivity by handling the variables with an integrated approach.

Author Statement

M. Serdar Çavuş: Conceptualization, Methodology, Theoretical Calculations, Formal Analysis, Investigation, Visualization.

Nesrin Şener: Conceptualization, Formal Analysis, Investigation, Resource/Material/Instrument Supply.

Acknowledgment

As the authors of this study, we declare that we do not have any support and thank you statement.

Conflict of Interest

As the authors of this study, we declare that we do not have any conflict of interest statement.

Ethics Committee Approval and Informed Consent

As the authors of this study, we declare that we do not have any ethics committee approval and/or informed consent statement.

References

[1] K. Venkataraman, *The chemistry of synthetic dyes* (Vol. 4), 2012, Elsevier.

[2] H. S. Freeman, A. T. Peters, *Colorants for non-textile applications*. 2000, Elsevier.

[3] Brown, J. "The chemistry of synthetic dyes used in cosmetics", *J Soc Cosmet Chem*, 18, 225-244, 1967.

[4] M. Kucharska, J. Grabka, "A review of chromatographic methods for determination of synthetic food dyes", *Pubmed*, Talanta, 80(3), 1045-1051, 2010.

[5] E. Gurr, *Synthetic dyes in biology, medicine and chemistry*, 2012, Elsevier.

[6] K.A. Naresh, R.C. Nagendranatha, P.R. Hari, M.S. Venkata, "Azo dye load-shock on relative behavior of biofilm and suspended growth configured periodic discontinuous batch mode operations: critical evaluation with enzymatic and bio-electrocatalytic analysis" *Water Res.* 60 (1), 182–196, 2014.

[7] Mark. Wainwright, "Dyes in the development of drugs and pharmaceuticals" *Dyes Pigments*, 76.3: 582-589, 2008.

[8] S. Rodriguez-Couto, "Enzymatic biotransformation of synthetic dyes" *Curr drug metab* 10.9: 1048-1054, 2009.

[9] F. Rafii, J. D. Hall, C. E. Cerniglia, "Mutagenicity of azo dyes used in foods, drugs and cosmetics before and after reduction by Clostridium species from the human intestinal tract." *Food Chem Toxicol* 35.9: 897-901, 1997.

[10] S. Erişkin, N. Şener, S. Yavuz, İ. Şener, "Synthesis, characterization, and biological activities of 4-imino-3-arylazo-4H-pyrimido [2, 1-b][1, 3] benzothiazole-2-oles", *Med Chem Res*, 23(8):3733–43,2014.
[11] N. Şener, İ. Şener, S. Yavuz, F. Karci," Synthesis, Absorption Properties and Biological Evaluation of Some Novel Disazo Dyes Derived from Pyrazole Derivatives", *Asian J Chem*, 27(8):3003–12, 2015.
[12] N. M. Mallikarjuna, J. Keshavayya, "Synthesis, spectroscopic characterization and pharmacological studies on novel sulfamethaxazole based azo dyes", *J King Saud Univ-Sci*, 32(1), 2018.
[13] M. A. Weaver, L. Shuttleworth, "Heterocyclic diazo component", *Dyes Pigments*, 3 (2,3), 81-121, 1982.
[14] K. Singh, S. Singh, J.A. Taylor, "Monoazo disperse dyes-part 1: synthesis, spectroscopic studies and technical evaluation of monoazo disperse dyes derived from 2-aminothiazoles", *Dyes Pigments*, 54, 189-200, 2002.
[15] K. Singh, S. Singh, A. Mahajan, A. Taylor, "Monoazo disperse dyes. Part 3: synthesis and fastness properties of some novel 4,5-disubstituted thiazolyl-2-azo disperse dyes", *Color Technol*, 119 (4), 198-204, 2003.
[16] S. Shibata, H. A. Flaschka, A. J. Barnard, *Chelates in Analytical Chemistry*, Vol. 4, Marcet Dekker, 1972, New York, 1st edn.
[17] G. Hallas, *J Soc Dyer Colorists*,95:285, 1979.
[18] D. W. Rangnekar, M. B. Chaudkari, *Dyes Pigments*, 10:173, 1989.
[19] T. G. Deligeorgiev, "An Improved method for the preparation of 2-aryl-, 2-hetaryl- and 2-styrylbenzothiazoles", *Dyes Pigments*, 12, 4, 243-248, 1990.
[20] A. Penchev, D. Simov, N. Gadjev, "Diazotization of 2-amino-6- methoxybenzothiazole at elevated temperature", *Dyes Pigments*, 16:77-81,1991.
[21] Peters AT, Gbadamosi NMA. *Dyes Pigments* 1992;18:115.
[22] N. M. Mallikarjuna, et al. "Synthesis, characterization, thermal and biological evaluation of Cu (II), Co (II) and Ni (II) complexes of azo dye ligand containing sulfamethaxazole moiety." *J Mol Struct*, 1165: 28-36, 2018.
[23] İ. Şener, N. Şener, M. Gür. "Synthesis, structural analysis, and absorption properties of disperse benzothiazol-derivative mono-azo dyes", *J Mol Struct*, 1174, Pages 12-17, 2018.
[24] N. M. Mallikarjuna, J. Keshavayya, "Synthesis, spectroscopic characterization and pharmacological studies on novel sulfamethaxazole based azo dyes", *J King Saud Univ* – Sci, 32, 251–259, 2020.
[25] F. Karcı, N. Şener, M. Yamaç, İ. Şener, A. Demirçalı, "The synthesis, antimicrobial activity and absorption characteristics of some novel heterocyclic disazo dyes", *Dyes Pigments*, 80(1), 47-52, 2009.
[26] N. Şener, S. Erişkin, S. Yavuz, İ. Şener, "Synthesis, Characterization, Solvatochromic Properties, and Antimicrobial- radical Scavenging Activities of New Diazo Dyes Derived from Pyrazolo [1, 5-a] pyrimidine", *J Heterocycl. Chem.*, 54(6), 3538-3548, 2017.
[27] S. M. Riyadh, A. A. Deawaly, H. E. Ahmed, T. H. Afifi, S. Ihmaid, "Novel arylazothiazoles and arylazo [1, 3, 4] thiadiazoles as potential antimicrobial and anticancer agents: synthesis, molecular modeling, and biological screening", *Med Chem Res*, 26(9), 1956-1968, 2017.
[28] F. Öztürk, L. Açik, İ. Şener, F. Karci, E. Kiliç, "Antimicrobial properties and DNA interactions studies of 3-hetarylazoquinoline-2, 4-diol compounds", *Turk J Chem*, 36(2):293–302, 2012.
[29] N. Şener, H. J. A. Mohammed, S. Yerlikaya, Y. C. Altunoglu, M. Gür, M. C. Baloglu, İ. Şener, "Anticancer, antimicrobial, and DNA protection analysis of novel 2, 4-dihydroxyquinoline dyes", *Dyes Pigments*, 157, 11-19, 2018.
[30] M. D. Engelmann, R. Hutcheson, I. F. Cheng, "Stability of Ferric Complexes with 3-Hydroxyflavone (Flavonol), 5, 7-Dihydroxyflavone (Chrysin), and 3 ', 4 '-Dihydroxyflavone", *J Agric Food Chem*, 53(8):2953–60, 2005.
[31] T. Thirunavukkarasu, H. A. Sparkes, K. Natarajan, "Quinoline based Pd (II) complexes: Synthesis, characterization and evaluation of DNA/protein binding, molecular docking and in vitro anticancer activity" *Inorganica Chim Acta*, 482, 229-239, 2018.
[32] PV Sri Ramya, et al. "Curcumin inspired 2-chloro/phenoxy quinoline analogues: Synthesis and biological evaluation as potential anticancer agents." *Bioorganic Med Chem Lett.*, 28.5, 892-898, 2018.
[33] X. Tian, et al. "Preparation of anticancer micro-medicine based on quinoline and chitosan with pH responsive release performance", *Colloids Surf B: Biointerfaces*, 165: 278-285, 2018.
[34] S. Kwon, et al. "Mitochondria-targeting indolizino [3, 2-c] quinolines as novel class of photosensitizers for photodynamic anticancer activity", *Eur J. Mel Chem.*, 148: 116-127, 2018.
[35] K. D. Upadhyay, et al. "Synthesis and Biological Screening of Pyrano [3, 2-c] quinoline Analogues as Anti-inflammatory and Anticancer Agents." *ACS Med Chem Lett.*, 9.3: 283-288, 2018.

[36] Y. Ma, F. Wang, S. Kambam, X. Chen, "A quinoline-based fluorescent chemosensor for distinguishing cadmium from zinc ions using cysteine as an auxiliary reagent", *Sensor Actuator B Chem*, 188:1116–22, 2013.
[37] E. M. Nolan, J. Jaworski, K-I Okamoto, Y. Hayashi, M. Sheng, S. J.Lippard, "QZ1 and QZ2: rapid, reversible quinoline-derivatized fluoresceins for sensing biological Zn (II)". *J Am Chem Soc*,127:16812–23, 2005.
[38] Z. Dong, Y. Guo, X. Tian, J. Ma, "Quinoline group based fluorescent sensor for detecting zinc ions in aqueous media and its logic gate behaviour", *J Lumin*, 134:635–9, 2013.
[39] S. Kobayashi, S. Nagayama, "A new methodology for combinatorial synthesis. Preparation of diverse quinoline derivatives using a novel polymer-supported scandium catalyst", *J Am Chem Soc*, 118(37), 8977-8978, 1996.
[40] J. P. Michael, "Quinoline, quinazoline and acridone alkaloids. Natural product reports", 24(1), 223-246, 2007.
[41] C. Dattatray, B. Priyabrata, at al., "n-alkylamino analogs of Vitamin K3: Electrochemical, DFT and anticancer activity of their oxidized and one electron reduced form", *J Mol Struct*, 1179 443-452, 2019.
[42] H. Iftikar, N. K. Gour, C. D. Ramesh, "Kinetics and thermochemistry of hydrolysis mechanism of a novelanticancer agent trans-[PtCl2(dimethylamine) (isopropylamine)]:A DFT study", *Chem Phys Lett*, 651: 216–220, 2016.
[43] J. J. M. Medina, at al., "Synthesis, characterization, theoretical studies and biological (antioxidant, anticancer, toxicity and neuroprotective) determinations of a copper(II) complex with 5-hydroxytryptophan", *Biomed & Pharmacother*, 111: 414–426, 2019.
[44] W. M. Al-Asbahy, at al., "A dinuclear copper(II) complex with piperazine bridge ligand as a potential anticancer agent: DFT computation and biological evaluation", *Inorganica Chim Acta,* 445: 167-178, 2016.
[45] N. T. Rahmouni, at al., "New mixed amino acids complexes of iron(III) and zinc(II) with isonitrosoacetophenone: Synthesis, spectral characterization, DFT study and anticancer activity", *Spectrochi Acta A: Mol and Biomol Spectrosc*, 213: 235–248, 2019.
[46] A. Spinello, A. Terenzi, G. Barone, "Metal complex–DNA binding: Insights from molecular dynamics and DFT/MM calculations", *J Inorg Biochem*, 124: 63–69, 2013.
[47] S. Baskaran, at al., "DFT analysis and DNA binding, cleavage of copper(II) complexes", *J Mol Liq*, 221: 1045–1053, 2016.
[48] B. Jadoo, at al., "Novel coumarin rhenium(I) and -(V) complexes: Formation, DFT and DNA binding studies", *Polyhedron*, 144: 107-118, 2018.
[49] S. I. Farooqi, at al., "Synthesis, theoretical, spectroscopic and electrochemical DNA binding investigations of 1, 3, 4-thiadiazole derivatives of ibuprofen and ciprofloxacin: Cancer cell line studies", *Journal of Photochem & Photobiolog*, B: Biology 189: 104–118, 2018.
[50] O. D. Okagu, at al., "Synthesis and characterization of Cu(II), Co(II) and Ni(II) complexes of a benzohydrazone derivative: Spectroscopic, DFT, antipathogenic and DNA binding studies", *J Mol Struct*, 1183: 107-117, 2019.
[51] Gaussian 09, Revision B.01, Frisch M. J, Trucks G. W, Schlegel H. B, Scuseria G. E, Robb M. A, Cheeseman J. R, Scalmani G., Barone V, Mennucci B, Petersson G. A, Nakatsuji H, Caricato M, Li X, Hratchian H. P, Izmaylov A. F, Bloino J, Zheng G, Sonnenberg J. L, Hada M, Ehara M, Toyota K, Fukuda R, Hasegawa J, Ishida M, Nakajima T, Honda Y, Kitao O, Nakai H, Vreven T, Montgomery J. A, Peralta J. E, Ogliaro F, Bearpark M, Heyd J. J, Brothers E, Kudin K. N, Staroverov V. N, Keith T, Kobayashi R, Normand J, Raghavachari K, Rendell A, Burant J. C, Iyengar S. S, Tomasi J, Cossi M, Rega N, Millam J. M, Klene M, Knox J. E, Cross J. B, Bakken V, Adamo C, Jaramillo J, Gomperts R, Stratmann R. E, Yazyev O, Austin A. J, Cammi R, Pomelli C, Ochterski J. W, Martin R. L, Morokuma K, Zakrzewski V. G, Voth G. A, Salvador P, Dannenberg J. J, Dapprich S, Daniels A. D, Farkas O, Foresman J. B, Ortiz J. V, Cioslowski J, Fox D. J, Gaussian, Inc., Wallingford CT, 2010.
[52] P. Hohenberg, W. Kohn, "Inhomogeneous Electron Gas", *Phys. Rev*., 136, B864, 1964.
[53] W. Kohn, L. Sham, "Self-Consistent Equations Including Exchange and Correlation Effects", *Phys. Rev*., 140, A1133, 1965.
[54] A. D Becke, "A new mixing of Hartree–Fock and local density- functional theories", *J Chem Phys*. 98, 1372, 1993.
[55] C. Lee, W. Yang, R.G. Parr, "Development of the Colle-Salvetti correlation-energy formula into a functional of the electron density", *Phys Rev B*, 37, 785, 1988.
[56] R. W. F. Bader, *Atoms in Molecules. A Quantum Theory*, Oxford: Calendon Press, 1990.

[57] R. F. W. Bader, ”Atoms in molecules”, *Acc. Chem. Res*. 18, 9, 1985.
[58] R. F. W. Bader,” A quantum theory of molecular structure and its applications” *Chem. Rev*., 91, 893, 1991.
[59] C. Reichart, T. Welton, *Solvent and Solvent Effect in Organic Chemistry*, Weinheim: Wiley-VCH Verlagand Co. KgaA, 2011, 4th Edn.
[60] Harikrishnan, U.; Menon, S. K., “Crown Ether Bis-diazo Dyes for Aqueous Inkjet Inks by Micro Emulsion Technique”, *Dyes Pigm*., 77, 462, 2008.
[61] B. Valeur, “Molecular Fluorescence: Principles and Applications”, 2012, Wiley-VCH: 357 Weinheim, Germany.